GMR Genetics and Molecular Research
Online Journal
ISSN:1676-5680

Gene expression profiles in the cerebellum of transgenic mice over expressing the human *FMR1* gene with CGG repeats in the normal range

J.J. Fernández[1], R. Martínez[1], E. Andújar[2], M. Pérez-Alegre[3], A. Costa[1], V. Bonilla-Henao[1], F. Sobrino[1], C.Ó. Pintado[4] and E. Pintado[1]

[1]Department of Medical Biochemistry and Molecular Biology, University Hospital Virgen Macarena, University of Seville, Spain
[2]Genomics Unit, Andalusian Molecular Biology and Regenerative Medicine Centre, CSIC, Seville, Spain
[3]Genomics Unit, Andalusian Molecular Biology and Regenerative Medicine Centre, Seville, Spain
[4]Breeding and Research Animal Center, University of Seville, Seville, Spain

Corresponding author: E. Pintado
E-mail: elizabet@us.es

Genet. Mol. Res. 11 (1): 467-483 (2012)
Received July 20, 2011
Accepted October 17, 2011
Published March 1, 2012
DOI http://dx.doi.org/10.4238/2012.March.1.4

ABSTRACT. Modifications in the GABA pathway are considered to be responsible for motor alterations in animal models for fragile X-associated tremor ataxia syndrome. We analyzed the expression profile in the cerebellum in a transgenic mouse model that over expresses the human *FMR1* gene with CGG repeats in the normal range. We used the "GeneChip Mouse Gene 1.0 ST Array" from Affymetrix analyzing 28,853 well-described and -characterized genes. Based on data from the comparative analysis of the expression profile, we detected a significant gradient with a P value <0.1 and changes in expression equal to or greater than 1.5 times compared to the control mouse genes. There were significant changes in the expression of 104 genes, among which 72% had decreased and 28% had increased expression. With the exception

of *GabarapL2*, no changes in expression of genes from the GABA pathway were observed, which may explain the absence of an altered motor phenotype in these mice. These results further support the view that toxic effects in fragile X-associated tremor ataxia syndrome are due to expansion of CGG repeats rather than increased mRNA levels, since in the transgenic mice the *FMR1* mRNA levels were increased 20-100 times compared with those of control littermates.

Key words: Animal model; Microarrays; *FMR1*; Cerebellum; FXTAS

INTRODUCTION

Loss of expression of the *FMR1* gene by increased CGG trinucleotide repeats (<200) in the 5'UTR causes the most frequent inherited form of mental retardation (fragile X syndrome, FXS), whereas carriers of premutation alleles (55-200 CGG triplet repeats) may present a specific late-onset neurodegenerative disorder characterized by tremor, ataxia, parkinsonism, and intellectual decline (fragile X-associated tremor ataxia syndrome, FXTAS) (Hagerman et al., 2001; Hagerman and Hagerman, 2004a; Jacquemont et al., 2007; Costa et al., 2011; Greco et al., 2011). Neurohistological studies on the brain of premutation carriers have demonstrated neuronal degeneration in the cerebellum and the presence of eosinophilic intranuclear inclusions in both neurons and astroglia (Jacquemont et al., 2003; Greco et al., 2006; Wenzel et al., 2010).

The increase in CGG repeats is parallel to an increase in *FMR1* mRNA levels without significant changes in *FMR1* mRNA stability (Kenneson et al., 2001; Loesch et al., 2007; Tassone et al., 2007). The knock-in mouse model generated in which the endogenous CGG repeat was replaced by a human CGG repeat in the premutation range displays biochemical, phenotypic and neuropathological characteristics of FXTAS (Willemsen et al., 2003). As in humans, the expanded CGG repeat mouse model shows elevated *fmr1* mRNA levels in the brain compared with controls (Willemsen et al., 2003; Brouwer et al., 2007; Hunsaker, 2011). The elevated level of this abnormal mRNA is believed to be the cause of the neurodegenerative disorder. In a *Drosophila* model expressing a portion of the premutated human *FMR1* 5'UTR the repeats may cause neurodegeneration in a dosage- and repeat length-dependent manner (Jin et al., 2003). An almost normal CGG repeat of 60 triplets, when moderately expressed, has little phenotype, and this same allele, when overexpressed, does lead to neurodegeneration, supporting the notion that overall rCGG abundance is critical for the pathological phenotype (Jin et al., 2003). The toxicity of the *FMR1* mRNA has been related to the excess recruitment of one or more RNA-binding proteins to the expanded repeats causing depletion and loss of function of these proteins (Hagerman and Hagerman, 2004b, 2007). Dysfunction in RNA metabolism has also been involved in the pathogenesis of several neurological disorders (Ginsberg et al. 1998; Gallo et al., 2005; Oostra and Willemsen, 2009; Lemmens et al., 2010).

It has been reported that overexpression of the *FMR1* gene with CGG in the normal range does not rescue the fragile X phenotype in KO mouse (Bakker et al., 2000) although a reversal of sensomotor gating abnormalities in the KO mice carrying a human *FMR1* transgene has been described (Paylor et al., 2008). However, a more detailed study of transgenic mice without CGG expansion is missing. To ascertain whether an increase in the *FMR1* mes-

senger level, independently of the CGG number, may affect the expression profile in cerebellum we performed a microarray analysis from a transgenic mouse model that overexpresses (20-100-fold) the human *FMR1* gene with CGG in the normal range.

MATERIAL AND METHODS

Animal models

The experiments were conducted in accordance with institutional guidelines and approved by the Animal Ethics Committee of the University of Seville. We generated a transgenic line that overexpresses human *FMR1* with CGG in the normal range (29 repeats). An *Eco*RI fragment containing the human *FMR1* cDNA kindly supplied by Dr. Verker (Erasmus Medical Center, Rotterdam, The Netherlands) was cloned in the *Eco*RI site of the expression vector pSG5. The plasmid plus the *FMR1* cDNA was grown in an LB broth buffer and the construction was cut with *Sal*I restriction enzyme. *Sal*I generates two fragments, one of 4.56 kb corresponding to the *FMR1* gene, T7 promoter, the β-globin intron and SV40 promoter and a fragment of 3.04 kb from the rest of the plasmid (Figure 1A).

The 4.56-kb fragment containing the *FMR1* cDNA was extracted from 0.8% agarose gel and purified with a kit from Qiagen (Qiagen Iberia, Madrid, Spain) (Figure 1B). A solution of 2.5 ng/µL containing the purified 4.56-kb fragment was microinjected into the pronucleus of fertilized murine oocytes as previously described (Mejias et al., 2006) and we selected two founder lines. DNA was extracted from mouse tissue by the QuickExtract™ DNA Extraction Solution 1.0 (Epicentric, Biotechnologies, Madison, WI, USA) and tested by conventional PCR of the KH domains with primers between exons 7 and 11 to prevent genomic DNA amplification as previously described (Hmadcha et al., 1998). The PCR was productive only in animals where the insert was incorporated in their genome (Figure 1C).

RNA extraction and quantitative RT-PCR

Cortex, cerebellum and liver tissues of transgenic mice and control littermates were dissected, placed immediately in TRIsure buffer and RNA was extracted as indicated by the manufacturer (Bioline, Luckenwalde, Germany). The concentration and quality of total RNA were analyzed spectrophotometrically. RNA was stored at -80°C until used. Reverse transcription (RT) reaction was performed in 40 µL with 0.5 to 1 µg total RNA, 1X PCR buffer, 5.5 mM $MgCl_2$, 1 mM each dNTP, 5 µM random primers, 0.4 RNAse inhibitor and 2.5 U M-MLV reverse transcriptase (Promega, Madison, WI, USA).

Quantitative (fluorescence) RT-PCR was performed in an ABI Prism 7300 Real-Time PCR System (Applied Biosystems, USA). PCRs were performed in triplicate in a total volume of 25 µL containing 100 ng cDNA and the SensiMix SYBR Green PCR master mix following the conditions recommended by the manufacturer (Quatance, London, UK). Primer sequences for human *FMR1* were from exon 3 and exon 5, FMR201F: 5'-GCAGATTCCATTTCAT GATGTCA-3', and FMR327R: 5'-CAATTGTGACAATTTCATTGTAAGTT-3' as described by Allen et al. (2004). For internal control, we used *hprt* gene expression assessed by using murine primers: hprtF: 5'-CACAGGACTAGAACACCTGC-3' and hprtR: 5'-GCTGGT GAAAAGGACCTCT-3' as described by Drabek et al. (1997).

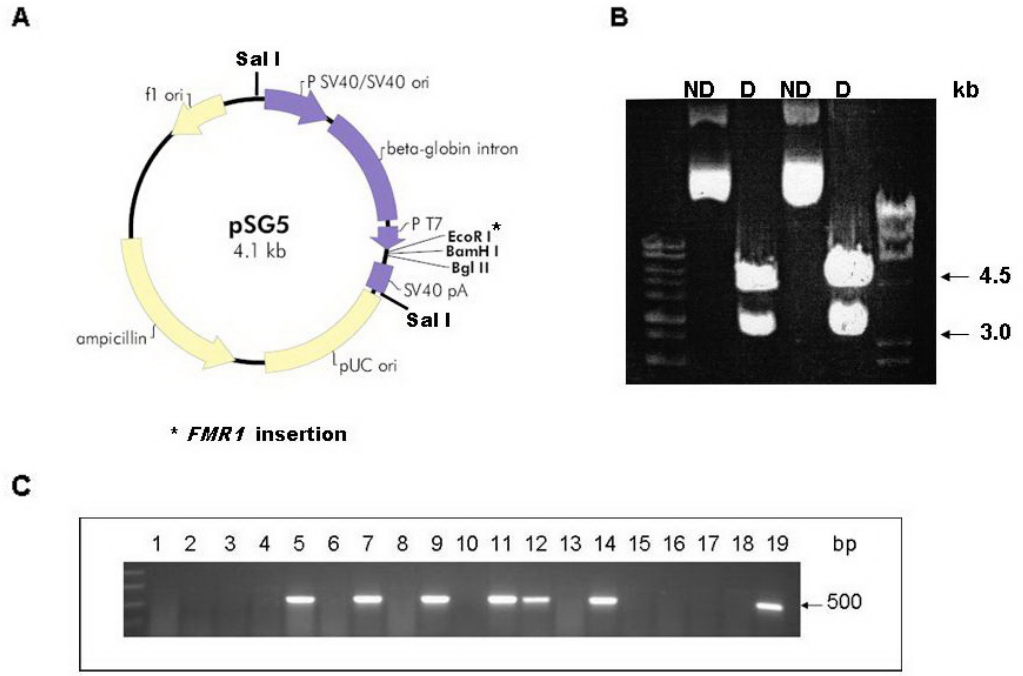

Figure 1. A. Scheme of the plasmid used to obtain the transgenic mice. The characteristics of the pSG5 plasmid are shown. The plasmid is cut with *Eco*RI where the cDNA of the human *FMR1* (3.5 kb) was inserted. The construct was incorporated into competent cells and grown in a medium with ampicillin. **B.** Plasmid extraction and digestion with *Sal*I. The plasmid was extracted with a kit from Quiagen and digested with the restriction enzyme *Sal*I. Two fragments of 4.561 and 3.039 kb were obtained. The 4.561-kb fragment contains *FMR1* cDNA, SV40 promoter and beta-globin intron. This fragment was separated on 0.8% agarose gel and purified. Dilutions were made for the injection in fertilized ovocites. *Lane ND* = plasmid non-digested; *lane D* = plasmid digested with *Sal*I. **C.** Detection of transgenic mice. Two founder lines were obtained (lines A and B). Genotyping was performed by conventional PCR of the KH domains and yielded a 500-bp fragment. Only animals that have incorporated the *FMR1* gene amplified the 500-bp fragment. Groups of both positive (+/-) and negative (-/-) mice of the same line and age were selected for the experiments. *Lanes 1*, *2*, *3*, *4*, *6*, *8*, *10*, *13*, *15*, *16*, *17*, and *18* = negative mice; *lanes 5*, *7*, *9*, *11*, *12*, and *14* = positive mice; *lane 19* = a positive control.

Quantitative RT-PCR amplification of c-fos was also performed in the ABI 7300 Real-time PCR System with gene-specific primers using the following sequences: *fos*F: 5'-CTGTCAACACACAGGACTTTT-3' and *fos*R: 5'-AGGAGATAGCTGCTCTACTTTG-3'. Glyceraldehyde-3-phosphate dehydrogenase (GAPDH) was used as an internal control, and was amplified using the following primers: GAPDH-F: 5'-CTTCACCACCATGGAGA AGGC-3' and GAPDH-R: 5'-GGCATGGACTGTGGTTCAT-3' as described by Janitzky et al. (2009). For all genes analyzed by quantitative RT-PCR the thermal cycle conditions consisted of initial denaturation at 95°C for 10 min followed by 40 cycles of 15 s at 95°C and 1 min at 60°C. Melting curve analysis showed a single sharp peak with the expected Tm for all samples. Determinations of cycle threshold were performed automatically by the instrument and calculations were done as described by Tassone et al. (2000a).

Microarray analysis

For microarray experiments RNA from transgenic mice and control littermates was extracted and maintained at 80°C until used. Gene expression profile was determined by using a "GeneChip Mouse Gene 1.0 ST Array" by Affymetrix platform at the Genomics Unit of CABIMER (Seville, Spain) containing 28,853 well-described and characterized genes. Quality of total RNA from mice was confirmed with Bioanalyzer® 2100 (Agilent technology). Synthesis, labeling and hybridization were performed with RNA from three independent mice of each condition following Affymetrix recommended protocols. Probe signal intensities were captured and processed with the GeneChip® Operating Software 1.4.0.036 (Affymetrix), and the resulting CEL files were reprocessed using robust multi-array average normalization (Irizarry et al., 2003). Fold change (log2) values and their P values were calculated with linear models for microarray analysis (Smyth, 2004), using the oneChannelGUI interface (Sanges et al., 2007). All statistical analyses were performed using R language and the packages freely available from the "Bioconductor Project" (http://www.bioconductor.org). With the data resulting from the comparative analysis of the expression profile, we established a significant grade with P value <0.1 and linear fold change in expression equal to or above 1.5 times above the control mouse. The functional annotation was analyzed using the DAVID Bioinformatics Database (http://david.abcc.ncifcrf.gov/home.jsp). The association of differentially expressed genes with genetic disorders and neurological diseases as well as hepatic diseases was identified using the IPA 9.0 software (Ingenuity Systems, www.ingenuity.com) available through the PAB (The Andalusian Platform of Bioinformatics www.scbi.uma.es) from the University of Malaga.

Assessment of exploration and activity

Open-field behavior was recorded in a brightly lit 50 x 50-cm arena. Mice always started from the center of the arena and were allowed 1 min of adaptation before the 60-min recording period commenced. A computerized video-tracking system (Smart.V2.5, Panlab, Barcelona, Spain) was used to record trajectories and calculate path length and time spent in the square periphery of the arena (Van Dam, 2005).

Statistical analysis

Exploration and activity data are presented as means ± SD, with the number (N) of experiments indicated. The statistical analysis of the data was performed using a non-parametric test. In particular, the Mann-Whitney U-test was used to check for statistical differences in distance covered and time spent in the periphery of the arena (PT%) between the control and the transgenic group. P values smaller than 0.1 were considered to be statistically significant.

RESULTS

We used the pronuclear injection of the 4.56-kb fragment to generate a transgenic mouse model that overexpresses human *FMR1* with CGG trinucleotide repeats in the normal range (29 repeats). Animals were genotyped by conventional PCR of the KH domain as in-

dicated in Material and Methods (see Figure 1C). Two founder lines, A and B, were obtained and positive (+/-) and negative (-/-) animals of the same age were maintained to perform the experiments.

Quantitative RT-PCR showed that the relative *FMR1* mRNA level in all tissues analyzed from transgenic mice was much higher than in the wild type. Figure 2 shows in bar diagrams the mean of three different experiments of *FMR1* mRNA levels in cerebellum, cortex and liver from mice at 14 weeks of age from line B. *FMR1* mRNA in the cerebellum of transgenic mice was 20 times higher than in the wild type, and the expression in cortex and liver tissue of transgenic mice was even higher compared to controls (50-100 times).

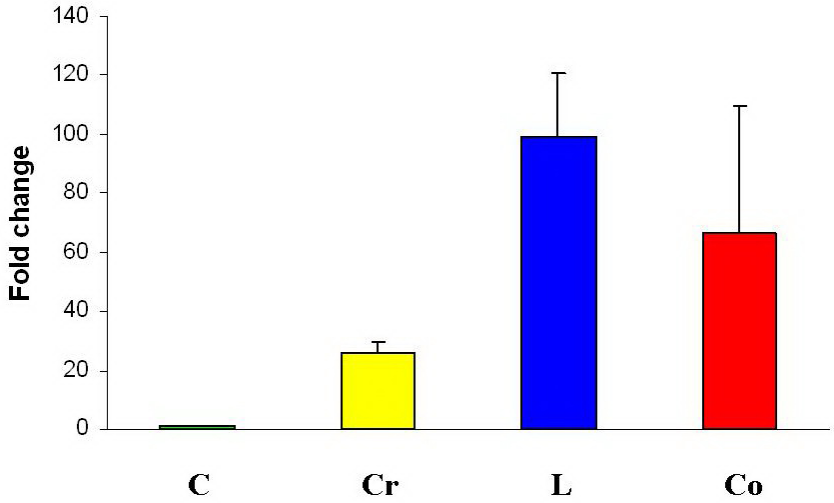

Figure 2. Quantitative RT-PCR of m*FMR1* in transgenic mice. Cerebellum (Cr), liver tissue (L) and cortex (Co) were dissected from transgenic and wild-type mice. RNA was isolated and reverse transcribed as indicated in Material and Methods. Real-time PCR showed that the expression of human *FMR1* was 20 to 100 times (fold change) higher than the values in control littermates, which were normalized to one (C). The results are reported as means ± SD of three different experiments from line B.

Behavioral analysis of male mice at 7 and 14 months did not show statistically significant differences between transgenic mice and control littermates (Table 1). The animals did not reveal significant differences in general activity or anxiety-related behaviors in the open-field test. Similar results were obtained using female mice of 3 and 11 months (data not shown).

Table 1. Assessment of exploration and activity.

	Wild type		Transgenic	
	Distance	PT%	Distance	PT%
7 months	13883 ± 5377 (6)	13.57 ± 5.7 (6)	12187 ± 2561 (6)	16.04 ± 7.43 (6)
14 months	11923 ± 4777 (4)	23.2 ± 4.73 (4)	11928 ± 2770 (4)	15.79 ± 11.18 (4)

Distance covered is reported in cm and permanence time (PT%) in percent of the total time spent in the periphery of the arena. Data are reported as means ± SD. Number of animals analyzed is indicated in parentheses.

For microarray analysis, we used transgenic mice of 20 weeks of age and control littermates. Considering the significant grade and linear changes in expression indicated in Material and Methods, we observed changes in 75 well-described genes in which 70% are inhibited and 30% increased by *FMR1* overexpression. Following the data supported by IPA 9.0 (see Material and Methods), we divided the changed genes into four categories including those related to neurological diseases and the GABAergic signaling pathway (Figure 3).

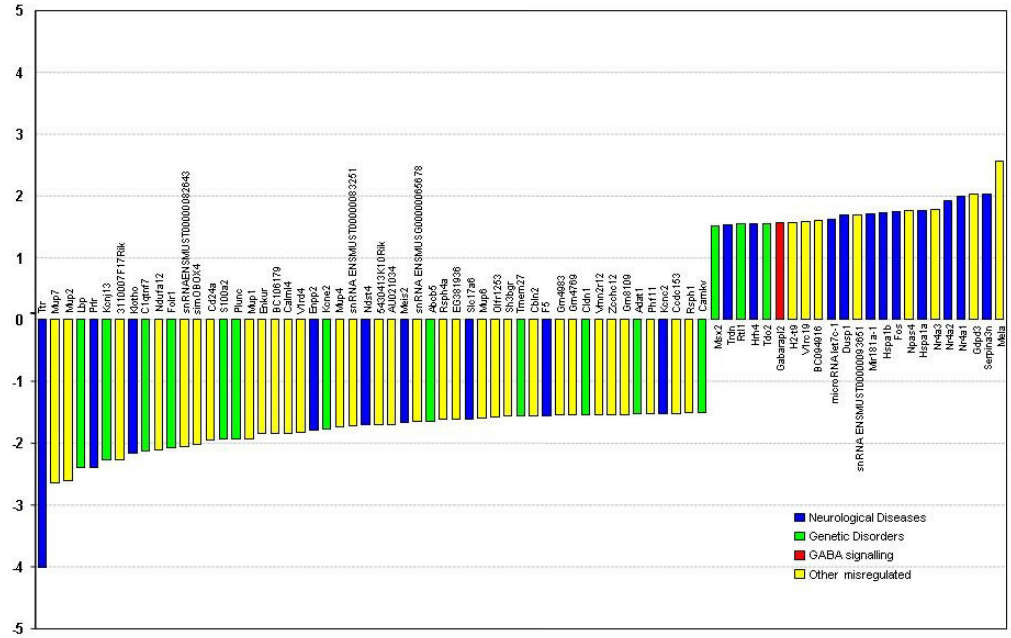

Figure 3. Gene expression profile in the cerebellum from transgenic mice. Cerebellar tissue was dissected and RNA was extracted as described in Material and Methods. cDNA was obtained by reverse transcription and expression was analyzed by "GeneChip Mouse ST 1.0 Array" manufactured by Affymetrix. The diagram shows the 75 well-characterized genes that present changes equal to or above 1.5 times with respect to control littermates and with a P value <0.1. From these genes 70% were inhibited (down in the graphic) and 30% were increased (up in the graphic). Genes related to neurological diseases are represented in blue, genes related to known genetic disorder in green and, other misregulated genes in yellow. With the exception of *GabarapL2* (red column) no known gene from the GABAergic pathway was altered.

Table 2 shows a detailed description of the 35 genes corresponding to the groups of neurological diseases (blue columns in Figure 3) and genetic disorders (green columns in Figure 3). A Veen diagram shows the genes shared by both groups and a subset of genes involved also in hepatic diseases.

The most affected gene is transthyretin (Ttr), a carrier of thyroxine and retinol that decreases four times compared with controls. On the other hand, Serpina3, a serine proteinase inhibitor (α-1-antichymotrypsin), is the most up-regulated gene from the neurological disease group. The data show that with the exception of the up-regulation of *GabarapL2* no change in expression of genes from the GABAergic pathway was observed. We have confirmed by real-time PCR the up regulation of cfos obtained in the microarray experiments (data not shown).

Table 2. Description and involvement in diseases of differentially expressed genes determined by microarray analysis in the cerebellum of transgenic mice versus wild type.

Symbol	Entrez Gene Name	Transcript ID	Source database	Entrez Gene ID	Cluster IPA assignment	Diseases
mir-181	microRNA 181a-1	NR_029795 /// mmu-mir-181a-1	RefSeq /// miRBase Micro RNA Database	735252	Genetic disorders, Neurological diseases, Hepatic system disease	Cancer, liver neoplasia, liver cancer, hepatocellular carcinoma, Alzheimer's disease, leiomyomatosis, leiomyoma, nonobstructive azoospermia, prostate cancer, prostatic carcinoma, breast cancer
F5	coagulation factor V (proaccelerin, labile factor)	ENSMUST0000008 6040 /// U52925 /// NM_007976	ENSEMBL /// GenBank /// RefSeq	14067	Genetic disorders, Neurological diseases	Thrombophilia, type I factor V deficiency, hematological neoplasia, acute respiratory distress syndrome, infection, stroke, severe sepsis, disseminated intravascular coagulation, acute pancreatitis, hypotension, septic shock, sepsis, coronary artery disease, ischemic stroke, Budd-Chiari syndrome, bipolar disorder, dengue hemorrhagic fever, thromboembolism, bacterial meningitis, bleeding, respiratory disorder, deep vein thrombosis, ischemic ardiomyopathy, thrombosis, bleeding disorder, cirrhosis, venous thrombosis
KCNJ13	potassium inwardly rectifying channel, subfamily J, member 13	ENSMUST0000011 3212 /// NM_001110227	ENSEMBL /// RefSeq	1E+08	Genetic disorders	Peripheral snowflake retinal degeneration
TRDN	triadin	NM_029726	RefSeq	76757	Genetic disorders, Neurological diseases	Bipolar disorder, non-insulin-dependent diabetes mellitus, coronary artery disease, hypertension
KCNC2	potassium voltage-gated channel, Shaw-related subfamily, member 2	ENSMUST0000009 2175 /// BC116289 /// NM_001025581	ENSEMBL /// GenBank /// RefSeq	268345	Genetic disorders, Neurological diseases	Non-insulin-dependent diabetes mellitus, epileptic seizure

Continued on next page

Table 2. Continued.

Symbol	Entrez Gene Name	Transcript ID	Source database	Entrez Gene ID	Cluster IPA assignment	Diseases
FOS	FBJ murine osteosarcoma viral oncogene homolog	ENSMUST0000002 1674 /// BC029814 /// NM_010234	ENSEMBL /// GenBank /// RefSeq	14281	Genetic disorders, Neurological diseases	Cancer, neoplasia, psoriasis, bone cancer, tumorigenesis, rheumatoid arthritis, endometriosis, seizures, kindling, experimental Huntington's disease, skin cancer, hyperplasia, alopecia, plaque psoriasis, inflammatory disorder, leiomyomatosis, uterine cancer, uterine leiomyoma, breast cancer, atherosclerosis, renal cancer, renal-cell carcinoma, osteolytic bone disease, multiple myeloma, polyarticular juvenile rheumatoid arthritis, hepatocellular carcinoma, coronary artery disease, hyperalgesia, liver neoplasia, liver cancer
SERPINA3	serpin peptidase inhibitor, clade A (alpha-1 antitrypsin), member 3	ENSMUST0000002 1506 /// M64086 /// NM_009252	ENSEMBL /// GenBank /// RefSeq	20716	Genetic disorders, Neurological diseases	Alzheimer's disease, rheumatoid arthritis, experimentally induced diabetes, antiproteinase, colon cancer, progressive supranuclear palsy, corticobasal degeneration, late-onset Alzheimer's disease, chronic fatigue syndrome, acute renal allograft rejection, Parkinson's disease, frontotemporal dementia with parkinsonism, Huntington's disease
RTL1	retrotransposon-like 1	ENSMUST0000014 9046 /// EU434918 /// NM_184109 /// NR_029550 /// mmu-mir-136	ENSEMBL /// GenBank /// RefSeq /// RefSeq /// miRBase Micro RNA Database	353326 /// 387154	Genetic disorders	Non-insulin-dependent diabetes mellitus
ABCB5	ATP-binding cassette, subfamily B (MDR/TAP), member 5	ENSMUST0000003 5515 // AY766239 /// NM_029961	ENSEMBL /// GenBank /// RefSeq	77706	Genetic disorders	Rheumatoid arthritis, coronary artery disease, non-Hodgkin's disease, multiple myeloma, acute myeloid leukemia, leukopenia, meningioma, primary biliary cirrhosis, brain cancer, glioblastoma, cancer

Continued on next page

Table 2. Continued.

Symbol	Entrez Gene Name	Transcript ID	Source database	Entrez Gene ID	Cluster IPA assignment	Diseases
MSX2	msh homeobox 2	ENSMUST0000002 1922 /// BC141132 /// NM_013601	ENSEMBL /// GenBank /// RefSeq	17702	Genetic disorders	Enlarged parietal foramina, parietal foramina cleidocranial dysplasia, pancreatic cancer, pancreatic carcinoma, nonsyndromic craniosynostosis
PRLR	prolactin receptor	ENSMUST0000012 4470 /// BC096586 /// NM_011169	ENSEMBL /// GenBank /// RefSeq	19116	Genetic disorders, Neurological diseases	Amyotrophic lateral sclerosis, Crohn's disease, cancer, endometritis, endometrial hyperplasia, mucinous ovarian cancer, mucinous ovarian carcinoma, clear-cell ovarian carcinoma, ovarian carcinoma, endometrioid carcinoma, uterine cancer, endometrial carcinoma, ovarian cancer, serous ovarian adenocarcinoma, medullary thyroid cancer, familial medullary thyroid cancer, thyroid cancer, head and neck cancer, neoplasia, tumorigenesis, hyperprolactinemia, insulin resistance, hyperglycemia, obesity, hypoinsulinemia, hyperleptinemia, hypoglycemia, experimentally induced adenomyosis, hypocalcemia
NR4A1	nuclear receptor subfamily 4, group A, member 1	ENSMUST0000002 3779 /// BC004770 /// NM_010444	ENSEMBL /// GenBank /// RefSeq	15370	Genetic disorders, Neurological diseases, Hepatic system disease	Huntington's disease, primary biliary cirrhosis, polyarticular juvenile rheumatoid arthritis, endometriosis, primary sclerosing cholangitis, osteoarthritis, dermatitis,
ENPP2	ectonucleotide pyrophosphatase/ phosphodiesterase 2	ENSMUST0000004 1591 /// BC058759 /// NM_015744	ENSEMBL /// GenBank /// RefSeq	18606	Genetic disorders, Neurological diseases, Hepatic system disease	Bipolar disorder, Crohn's disease, rheumatoid arthritis, metastasis, Rett syndrome, tuberculoid leprosy, chronic fatigue syndrome, metastatic colorectal cancer, hepatocellular carcinoma, liver neoplasia, liver cancer, cancer
let-7	microRNA let-7b	NR_029728 /// mmu-let-7c-1	RefSeq /// miRBase Micro RNA Database	387246	Genetic disorders, Neurological diseases, Hepatic system disease	Cancer, breast cancer, liver neoplasia, liver cancer, hepatocellular carcinoma, infection by *Cryptosporidium parvum*, Alzheimer's disease, nonobstructive azoospermia, schizophrenia, lung cancer, lung squamous cell carcinoma, limb girdle muscular dystrophy type 2B, melanoma metastases, squamous-cell carcinoma, limb girdle muscular dystrophy type 2A, facioscapulohumeral muscular dystrophy, nemaline myopathy, melanoma, Miyoshi myopathy, leiomyomatosis, leiomyoma, Down's syndrome, prostate cancer, prostatic carcinoma, breast carcinoma, metastasis

Continued on next page

Table 2. Continued.

Symbol	Entrez Gene Name	Transcript ID	Source database	Entrez Gene ID	Cluster IPA assignment	Diseases
KCNE2	potassium voltage-gated channel, Isk-related family, member 2	ENSMUST0000004 7383 /// BC022699 /// NM_134110	ENSEMBL /// GenBank /// RefSeq	246133	Genetic disorders	Angina pectoris, acute myocardial infarction, congestive heart failure, lung cancer, atrial fibrillation, ventricular fibrillation, ventricular tachycardia, ventricular arrhythmia, atrial fibrillation, familial, long qt syndrome variant 3, hypochlorhydria, achlorhydria, hypergastrinemia, hyperplasia
CLDN1	claudin 1	ENSMUST0000002 3154 /// BC002003 /// NM_016674	ENSEMBL /// GenBank /// RefSeq	12737	Genetic disorders	Coronary artery disease, NISCH syndrome, breast cancer, colon cancer
DUSP1	dual specificity phosphatase 1	ENSMUST0000002 5025 /// BC006967 /// NM_013642	ENSEMBL /// GenBank /// RefSeq	19252	Genetic disorders, Neurological diseases, Hepatic system disease	Hypertrophy, flu, endometriosis, prostatic carcinoma, leiomyomatosis, leiomyoma, experimentally induced diabetes, collagen-induced arthritis, weight loss, atopic dermatitis, psoriasis, breast cancer, rheumatoid arthritis, prostate cancer, experimental autoimmune encephalomyelitis
HSPA1A/ HSPA1B	heat shock 70-kDa protein 1A	ENSMUST0000008 7328 /// BC054782 /// NM_010479	ENSEMBL /// GenBank /// RefSeq	193740	Genetic disorders, Neurological diseases	Huntington's disease, insulin-dependent diabetes mellitus, cancer, Alzheimer's disease, hepatocellular carcinoma, schizophrenia, liver neoplasia, liver cancer, obesity, neurodegeneration, bladder cancer, bladder carcinoma, experimental colitis, acidosis, adrenoleukodystrophy, polyarticular juvenile rheumatoid arthritis, endometriosis, amyotrophic lateral sclerosis, weight loss, tumorigenesis, hyperplasia, Parkinson's disease, ischemia, tremor, hypertrophy
HRH4	histamine receptor H4	ENSMUST0000004 1676 /// AF358859 /// NM_153087	ENSEMBL /// GenBank /// RefSeq	225192	Genetic disorders, Neurological diseases	Vomiting, metastatic breast cancer, urticaria, motion sickness, nausea, coronary artery disease, breast carcinoma
TTR	transthyretin	ENSMUST0000007 5312 /// D89076 /// NM_013697	ENSEMBL /// GenBank /// RefSeq	22139	Genetic disorders, Neurological diseases, Hepatic system disease	Alzheimer's disease, amyloidosis, neurological disorder, senile systemic amyloidosis, systemic reactive amyloidosis, familial amyloidotic polyneuropathy, hepatic system disorder, cancer, lung cancer, bronchiolo-alveolar adenocarcinoma, first-onset paranoid schizophrenia, cold thyroid nodule, major depression, experimentally induced diabetes

Continued on next page

Table 2. Continued.

Symbol	Entrez Gene Name	Transcript ID	Source database	Entrez Gene ID	Cluster IPA assignment	Diseases
PLUNC	palate, lung and nasal epithelium associated	ENSMUST0000002 8985 /// BC054375 /// NC_013697	ENSEMBL /// GenBank /// RefSeq	18843	Genetic disorders	Non-small cell lung cancer, non-small cell lung carcinoma, lung cancer, lung adenocarcinoma, cancer
LBP	lipopolysaccharide binding protein	ENSMUST0000001 6168 /// BC004795 /// NM_008489	ENSEMBL /// GenBank /// RefSeq	16803	Genetic disorders, Hepatic system disease	Non-insulin-dependent diabetes mellitus, coronary artery disease, hypertension, progressive familial intrahepatic cholestasis type 1, liver cancer, Crohn's disease, pneumonia, sepsis, rheumatoid arthritis, hepatic steatosis, pneumococcal pneumonia, experimental colitis, bacterial pneumonia
NR4A2	nuclear receptor subfamily 4, group A, member 2	ENSMUST0000011 2629 /// BC137715 /// NM_013613 NM_001139509	ENSEMBL /// GenBank /// RefSeq /// RefSeq	18227	Genetic disorders, Neurological diseases	Familial Parkinson's disease, atopic dermatitis, progressive supranuclear palsy, polyarticular juvenile rheumatoid arthritis, psychosis, T-cell non-Hodgkin's disease, peripheral T-cell lymphoma, Parkinson's disease, breast cancer, osteoarthritis, psoriasis
MEIS2	Meis homeobox 2	ENSMUST0000014 9217 /// U57343 /// NM_010825 ///	ENSEMBL /// GenBank /// RefSeq	17536	Genetic disorders, Neurological diseases	Hypertension, insulin-dependent diabetes mellitus, Huntington's disease, autosomal dominant polycystic kidney disease
S100A2	S100 calcium binding protein A2	GENSCAN0000001 6041 /// XM_001478157 /// XM_910611	ENSEMBL /// RefSeq /// RefSeq	628324	Genetic disorders	Psoriasis, serous ovarian carcinoma process, serous ovarian carcinoma, delayed hypersensitive reaction, lichen planus, endometrioid carcinoma, breast cancer, atopic dermatitis, ovarian cancer, clear-cell ovarian carcinoma, mucinous ovarian cancer, mucinous ovarian carcinoma, cancer
NDST4	N-deacetylase/N-sulfotransferase (heparan glucosaminyl) 4	ENSMUST0000014 3461 /// AB036838 /// NM_022565	ENSEMBL /// GenBank /// RefSeq	64580	Genetic disorders, Neurological diseases	Alzheimer's disease
TDO2	tryptophan 2,3-dioxygenase	ENSMUST0000002 9645 /// BC018390 /// NM_019911	ENSEMBL /// GenBank /// RefSeq	56720	Genetic disorders, Hepatic system disease	Crohn's disease, liver cancer, cancer, esophageal cancer, esophageal adenocarcinoma, Barrett's syndrome
C1QTNF7	C1q and tumor necrosis factor-related protein 7	ENSMUST0000007 6939 /// BC090967 /// NM_175425 /// NM_001135172	ENSEMBL /// GenBank /// RefSeq /// RefSeq	109323	Genetic disorders	Crohn's disease

Continued on next page

Table 2. Continued.

Symbol	Entrez Gene Name	Transcript ID	Source database	Entrez Gene ID	Cluster IPA assignment	Diseases
KL	klotho	ENSMUST0000007 8856 /// AB005141 /// NM_013823	ENSEMBL /// GenBank /// RefSeq	16591	Genetic disorders, Neurological diseases	Amyotrophic lateral sclerosis, spontaneous hypertension, arteriosclerosis, hyperplasia, osteoporosis, pulmonary emphysema, hyperphosphatemia, rheumatoid arthritis, tumoral calcinosis, osteoarthritis, X-linked hypophosphatemia
SLC17A6	solute carrier family 17 (sodium-dependent inorganic phosphate cotransporter), member 6	ENSMUST0000003 2710 /// BC038375 /// NM_080853	ENSEMBL /// GenBank /// RefSeq	140919	Genetic disorders, Neurological diseases	Parkinson's disease
FOLR1	folate receptor 1 (adult)	ENSMUST0000010 6986 /// AF096319 /// NM_008034	ENSEMBL /// GenBank /// RefSeq	14275	Genetic disorders	Coronary artery disease, infection by Ebola virus, infection by Marburg virus, infection, endometrioid carcinoma, ovarian cancer, clear-cell ovarian carcinoma, serous ovarian carcinoma process, serous ovarian carcinoma, mucinous ovarian cancer, mucinous ovarian carcinoma, neoplasia, tumorigenesis, pituitary gland adenoma, cancer, infection by HIV
Gabarapl2	GABA(A) receptor-associated protein-like 2	ENSMUST0000003 4428	ENSEMBL	93739	Genetic disorders	Coronary artery disease, productive infection by HIV-1, infection by HIV-1
ADAT1	adenosine deaminase, tRNA-specific 1	ENSMUST0000003 4427 /// AF192375 /// NM_013925	ENSEMBL /// GenBank /// RefSeq	30947	Genetic disorders	Coronary artery disease, non-insulin-dependent diabetes mellitus
CAMKV	CaM kinase-like vesicle-associated	ENSMUST0000003 5700 /// BC11103 /// NM_145621	ENSEMBL /// GenBank /// RefSeq	235604	Genetic disorders	Crohn's disease
TMEM27	transmembrane protein 27	ENSMUST0000011 2280 BC049912 /// NM_020626	ENSEMBL /// GenBank /// RefSeq	57394	Genetic disorders	Lung cancer, bronchiolo-alveolar adenocarcinoma, cancer

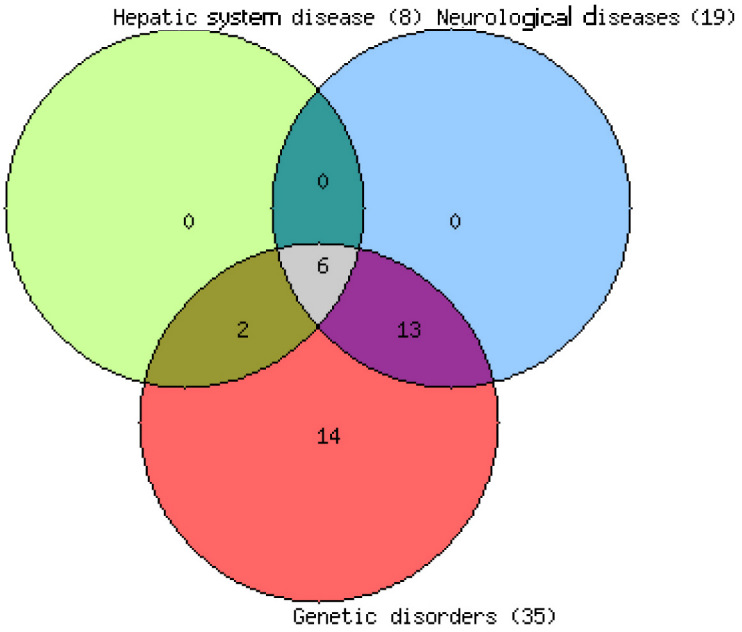

Venn diagram. Intersection of genes from different groups. The criteria used to define candidate differentially expressed genes are indicated in Material and Methods. Genes from "Other misregulted" group (yellow columns in Figure 3) are not described.

These results indicate that the increase in the expression of human *FMR1* mRNA with CGG triplets in the normal range in mice produced mild changes in the transcriptome but did not affect the GABAergic pathway or induce the motor alterations described in the animal model of FXTAS. The possible significance of the altered gene expression profile in the transgenic mice reported here should be further analyzed.

DISCUSSION

The involvement of the GABAergic system in both FXS and FXTAS, the two faces of the *FMR1* gene, has been reported (D'Hulst et al., 2009). Expression analysis of *fmr1* KO mice compared to wild type shows decreased expression of several subunits of the $GABA_A$ receptor in fragile X mouse cortex, but not in cerebellum. By contrast overexpression of several $GABA_A$ receptor subunits and proteins involved in GABA metabolism has been observed in cerebellum but not in the cortex of the mice model for FXTAS (D'Hulst et al., 2009). This is consistent with the cerebellar phenotype of FXTAS patients (D'Hulst et al., 2009) although the precise mechanistic relationship between CGG size and clinical phenotype is still unclear. It is likely that a combination of CGG repeat length and *FMR1* message abundance together may define a threshold for the clinical manifestation of the disease (Jin et al., 2003; Willemsen et al., 2003; Brouwer et al., 2007). In our transgenic mice expression of human *FMR1* mRNA is 20 to 100 times higher than in controls in any tissue analyzed (see Figure 2). These levels are an order of magnitude higher than the 2-6-fold elevated *FMR1* mRNA levels found in

premutation carriers or in the transgenic CGG-expanded repeat mouse model (Tassone et al., 2000a; Willemsen et al., 2003).

The high expression of human *FMR1* mRNA results in a differential expression pattern in cerebellum but only the *GabarapL2* gene from the GABAergic pathway was changed. According to these results, we did not find any motor phenotype in males or females at different ages (see Table 1). These data agree with the absence of correlation between *Fmr1* mRNA levels and neuropathological features found in the CGG-repeat knock-in mouse model (Brouwer et al., 2008). This study further supports the view that gain-of-function in FXTAS arises as a result of the expanded CGG repeats rather than the abnormally increased levels of *FMR1* mRNA present in a carrier of premutation alleles. Therefore, it would be of interest to know if fragile X males with unmethylayed full-mutation trinucleotide repeat expansions (Tassone et al., 2000b) show a severe form of FXTAS or an early presentation due to the very large CGG repeat expansion.

Interestingly, the two most altered genes from the group of neurological diseases, Trt and Serpina 3, found in our transgenic mice, are related to Alzheimer disease. A decrease in TRT has been associated with late onset Alzheimer disease and it is used in cerebrospinal fluid as a bio-marker (Buxbaum et al., 2008). On the other hand, up-regulation of Serpina 3 is found in Alzheimer patients (Porcellini et al., 2008). Thus, this may suggest an RNA toxicity that would work through alteration of specific genes. A subgroup of modified gene expression is related to hepatic diseases (see Venn diagram and Table 2). Since the transgenic mice reported here express extremely high *FMR1* mRNA levels in liver it would be of interest to know the gene expression profile of this tissue and its correlation with a possible hepatic phenotype.

The increase in c-fos proto-oncogene observed in the microarray has been validated by quantitative RT-PCR. However, *Fmr1* mRNA was not changed in the microarray analysis due to specific amplification of mouse *Fmr1* without recognition of human *FMR1* cDNA.

In conclusion, differential expression of genes determined by microarray analysis from transgenic mice versus wild type did not induce changes in the GABAergic system and transgenic mice did not show a cerebellar phenotype. The changes in the transcriptome may produce a non-cerebellar phenotype that should be further investigated.

ACKNOWLEDGMENTS

We would like to thank Dr. Verker for kindly supplying the human FMR1 cDNA. We also thank Dr. López-Barneo for critical reading of the manuscript. Research supported by a Grant from the Instituto de Salud Carlos III, Ministerio de Educación y Ciencia de España (#PI081332). J.J. Fernández was supported by a fellowship from the Hospital Universitario Virgen Macarena de Sevilla.

REFERENCES

Allen EG, He W, Yadav-Shah M and Sherman SL (2004). A study of the distributional characteristics of FMR1 transcript levels in 238 individuals. *Hum. Genet.* 114: 439-447.

Bakker CE, Kooy RF, D'Hooge R and Tamanini F (2000). Introduction of a *FMR1* transgene in the fragile X knockout mouse. *Neurosc. Res. Communic.* 26: 265-277.

Brouwer JR, Mientjes EJ, Bakker CE, Nieuwenhuizen IM, et al. (2007). Elevated Fmr1 mRNA levels and reduced protein expression in a mouse model with an unmethylated fragile X full mutation. *Exp. Cell Res.* 313: 244-253.

Brouwer JR, Huizer K, Severijnen LA, Hukema RK, et al. (2008). CGG-repeat length and neuropathological and molecular correlates in a mouse model for fragile X-associated tremor/ataxia syndrome. *J. Neurochem.* 107: 1671-1682.

Buxbaum JN, Ye Z, Reixach N, Friske L, et al. (2008). Transthyretin protects Alzheimer's mice from the behavioral and biochemical effects of Aβ toxicity. *Proc. Natl. Acad. Sci. U. S. A.* 105: 2681-2686.

Costa A, Gao L, Carrillo F, Caceres-Redondo MT, et al. (2011). Intermediate alleles at the *FRAXA* and *FRAXE* loci in Parkinson's disease. *Parkinsonism Relat. Disord.* 17: 281-284.

D'Hulst C, Heulens I, Brouwer JR, Willemsen R, et al. (2009). Expression of the GABAergic system in animal models for fragile X syndrome and fragile X associated tremor/ataxia syndrome (FXTAS). *Brain Res.* 1253: 176-183.

Drabek D, Raguz S, De Wit TP, Dingjan GM, et al. (1997). Correction of the X-linked immunodeficiency phenotype by transgenic expression of human Bruton tyrosine kinase under the control of the class II major histocompatibility complex Ea locus control region. *Proc. Natl. Acad. Sci. U. S. A.* 94: 610-615.

Gallo JM, Jin P, Thornton CA, Lin H, et al. (2005). The role of RNA and RNA processing in neurodegeneration. *J. Neurosci.* 25: 10372-10375.

Ginsberg SD, Galvin JE, Chiu TS, Lee VM, et al. (1998). RNA sequestration to pathological lesions of neurodegenerative diseases. *Acta Neuropathol.* 96: 487-494.

Greco CM, Berman RF, Martin RM, Tassone F, et al. (2006). Neuropathology of fragile X-associated tremor/ataxia syndrome (FXTAS). *Brain* 129: 243-255.

Greco CM, Navarro CS, Hunsaker MR, Maezawa I, et al. (2011). Neuropathologic features in the hippocampus and cerebellum of three older men with fragile X syndrome. *Mol. Autism* 2: 2.

Hagerman PJ and Hagerman RJ (2004a). Fragile X-associated tremor/ataxia syndrome (FXTAS). *Ment. Retard. Dev. Disabil. Res. Rev.* 10: 25-30.

Hagerman PJ and Hagerman RJ (2004b). The fragile-X premutation: a maturing perspective. *Am. J. Hum. Genet.* 74: 805-816.

Hagerman PJ and Hagerman RJ (2007). Fragile X-associated tremor/ataxia syndrome - an older face of the fragile X gene. *Nat. Clin. Pract. Neurol.* 3: 107-112.

Hagerman RJ, Leehey M, Heinrichs W, Tassone F, et al. (2001). Intention tremor, parkinsonism, and generalized brain atrophy in male carriers of fragile X. *Neurology* 57: 127-130.

Hmadcha A, De Diego Y and Pintado E (1998). Assessment of FMR1 expression by reverse transcriptase-polymerase chain reaction of KH domains. *J. Lab. Clin. Med.* 131: 170-173.

Hunsaker MR, von Leden RE, Ta BT, Goodrich-Hunsaker NJ, et al. (2011). Motor deficits on a ladder rung task in male and female adolescent and adult CGG knock-in mice. *Behav. Brain Res.* 222: 117-121.

Irizarry RA, Hobbs B, Collin F, Beazer-Barclay YD, et al. (2003). Exploration, normalization, and summaries of high density oligonucleotide array probe level data. *Biostatistics* 4: 249-264.

Jacquemont S, Hagerman RJ, Leehey M, Grigsby J, et al. (2003). Fragile X premutation tremor/ataxia syndrome: molecular, clinical, and neuroimaging correlates. *Am. J. Hum. Genet.* 72: 869-878.

Jacquemont S, Hagerman RJ, Hagerman PJ and Leehey MA (2007). Fragile-X syndrome and fragile X-associated tremor/ataxia syndrome: two faces of FMR1. *Lancet Neurol.* 6: 45-55.

Janitzky K, Stork O, Lux A, Yanagawa Y, et al. (2009). Behavioral effects and pattern of brain c-fos mRNA induced by 2,5-dihydro-2,4,5-trimethylthiazoline, a component of fox feces odor in GAD67-GFP knock-in C57BL/6 mice. *Behav. Brain Res.* 202: 218-224.

Jin P, Zarnescu DC, Zhang F, Pearson CE, et al. (2003). RNA-mediated neurodegeneration caused by the fragile X premutation rCGG repeats in *Drosophila*. *Neuron* 39: 739-747.

Kenneson A, Zhang F, Hagedorn CH and Warren ST (2001). Reduced FMRP and increased FMR1 transcription is proportionally associated with CGG repeat number in intermediate-length and premutation carriers. *Hum. Mol. Genet.* 10: 1449-1454.

Lemmens R, Moore MJ, Al-Chalabi A, Brown RH Jr, et al. (2010). RNA metabolism and the pathogenesis of motor neuron diseases. *Trends Neurosci.* 33: 249-258.

Loesch DZ, Bui QM, Huggins RM, Mitchell RJ, et al. (2007). Transcript levels of the intermediate size or grey zone fragile X mental retardation 1 alleles are raised, and correlate with the number of CGG repeats. *J. Med. Genet.* 44: 200-204.

Mejias R, Villadiego J, Pintado CO, Vime PJ, et al. (2006). Neuroprotection by transgenic expression of glucose-6-phosphate dehydrogenase in dopaminergic nigrostriatal neurons of mice. *J. Neurosci.* 26: 4500-4508.

Oostra BA and Willemsen R (2009). FMR1: a gene with three faces. *Biochim. Biophys. Acta* 1790: 467-477.

Paylor R, Yuva-Paylor LA, Nelson DL and Spencer CM (2008). Reversal of sensorimotor gating abnormalities in Fmr1 knockout mice carrying a human Fmr1 transgene. *Behav. Neurosci.* 122: 1371-1377.

Porcellini E, Davis EJ, Chiappelli M, Ianni E, et al. (2008). Elevated plasma levels of alpha-1-anti-chymotrypsin in age-related cognitive decline and Alzheimer's disease: a potential therapeutic target. *Curr. Pharm. Des.* 14: 2659-2664.

Sanges R, Cordero F and Calogero RA (2007). oneChannelGUI: a graphical interface to Bioconductor tools, designed for life scientists who are not familiar with R language. *Bioinformatics* 23: 3406-3408.

Smyth GK (2004). Linear models and empirical Bayes methods for assessing differential expression in microarray experiments. *Stat. Appl. Genet. Mol. Biol.* 3: Article3.

Tassone F, Hagerman RJ, Taylor AK, Gane LW, et al. (2000a). Elevated levels of FMR1 mRNA in carrier males: a new mechanism of involvement in the fragile-X syndrome. *Am. J. Hum. Genet.* 66: 6-15.

Tassone F, Hagerman RJ, Loesch DZ, Lachiewicz A, et al. (2000b). Fragile X males with unmethylated, full mutation trinucleotide repeat expansions have elevated levels of FMR1 messenger RNA. *Am. J. Med. Genet.* 94: 232-236.

Tassone F, Beilina A, Carosi C, Albertosi S, et al. (2007). Elevated FMR1 mRNA in premutation carriers is due to increased transcription. *RNA* 13: 555-562.

Van Dam D, Errijgers V, Kooy RF, Willemsen R, et al. (2005). Cognitive decline, neuromotor and behavioural disturbances in a mouse model for fragile-X-associated tremor/ataxia syndrome (FXTAS). *Behav. Brain Res.* 162: 233-239.

Wenzel HJ, Hunsaker MR, Greco CM, Willemsen R, et al. (2010). Ubiquitin-positive intranuclear inclusions in neuronal and glial cells in a mouse model of the fragile X premutation. *Brain Res.* 1318: 155-166.

Willemsen R, Hoogeveen-Westerveld M, Reis S, Holstege J, et al. (2003). The FMR1 CGG repeat mouse displays ubiquitin-positive intranuclear neuronal inclusions; implications for the cerebellar tremor/ataxia syndrome. *Hum. Mol. Genet.* 12: 949-959.